

Atomic mechanism for dislocation emission from nanosized grain boundaries

H. Van Swygenhoven, P. M. Derlet, and A. Hasnaoui
Paul Scherrer Institute, Villigen, CH-5232, Switzerland
 (Received 22 February 2002; published 24 June 2002)

The present work deals with the atomic mechanism responsible for the emission of partial dislocations from grain boundaries (GB's) in nanocrystalline metals. It is shown that in 12 and 20 nm grain size samples GB's containing GB dislocations can emit a partial dislocation during deformation by local atomic shuffling and stress-assisted free volume migration. The free volume is often emitted or absorbed in a neighboring triple junction. It is further suggested that the degree of delocalization surrounding the grain boundary dislocation determines whether atomic shuffling can associate displacements into the Burgers vector necessary to emit a partial dislocation. Temporal analysis of atomic configurations during dislocation emission indicates that creation and propagation of the partial might be separate processes.

DOI: 10.1103/PhysRevB.66.024101

PACS number(s): 62.25.+g, 87.64.Aa, 61.72.Mm, 61.72.Bb

I. INTRODUCTION

For some polycrystalline metals with grain sizes in the nanoregime, experiments have suggested a deviation away from the Hall-Petch relation^{1,2} relating yield stress to average grain size.³ The debate continues whether or not such deviations are a result of intrinsically different material properties of nanocrystalline (nc) systems or due simply to inherent difficulties in the preparation of fully dense nc samples and in their microstructural characterization. Nevertheless, it suggests that the traditional work hardening mechanism of pileup of dislocations originating from Frank-Read sources may no longer be valid at the nanometer scale. *In situ* deformation testing in a transmission electron microscope (TEM), performed on Cu and Ni₃Al nc samples, reveals a limited dislocation activity in grains below 50 nm.^{4,5} However, due to the presence of large internal stresses, which makes grain boundaries (GB's) in TEM images difficult to observe, and also possible artifacts induced by thin-film geometry such as dislocations emitted from the surface,⁶ the issue of dislocation activity remains a heavily discussed matter.

The use of large scale molecular dynamics (MD) in the study of the mechanical properties of nc materials provides a detailed picture of the atomic-scale processes during plastic deformation at room temperature.⁷⁻¹⁷ The primary observation of this simulation work has been the observed transition, with increasing grain size, from an entirely intergranular plastic deformation mechanism based on grain boundary sliding (GBS), to one which consists of both grain boundary accommodation mechanisms and the intragranular deformation process consisting of dislocation activity. MD performed at room temperature suggests that the GB accommodation mechanism can be identified with GB sliding triggered by atomic shuffling and to some extent stress assisted diffusion.^{9,10} On the other hand, MD performed at temperatures above $0.7T_m$ by Yamakov *et al.*^{14,15} suggest a Coble creep mechanism; in other words, the GB sliding is governed by GB diffusion. These authors further suggest an extrapolation of Coble creep to room temperatures. There is, however, no real justification for such an extrapolation since one can in no way assume that the rate limiting process close to the melting temperature remains dominant at room temperature.

Indeed, even for the simpler case of unassisted GB diffusion, there exists for a general GB network no detailed MD study of the corresponding atomic-scale activity as a function of temperature.

At larger grain sizes, dislocation activity is observed. In fully three-dimensional (3D) GB networks, which have been modeled now up to 20 nm grain sizes, only partial dislocations have been observed. They are always emitted from the GB's, often close to triple junctions. In the work of Yamakov *et al.*,¹⁶ full dislocations have been observed in 2D columnar network structures with columnar diameters up to 70 nm.

It is the aim of the present work to reveal atomic mechanisms responsible for the emission of the partials from the GB's. It is shown that in the observed cases, a GB dislocation dissociates into a partial lattice dislocation, meanwhile changing the grain boundary structure and its dislocation distribution. This mechanism is the reverse of what is often observed during absorption of a lattice dislocation, where the impinging dislocation is fully or partially absorbed in the GB, creating local changes in the structure and GB dislocation network.¹⁸

II. SAMPLE PREPARATION

Nanocrystalline samples are created using the Voronoi construction¹⁹ with random nucleated seeds and random crystallographic orientations. The sample is then relaxed to a minimum enthalpy at 300 K for 100 ps using isokinetic molecular dynamics. For the 12 nm sample, the relaxed structure has a final density of 97% of the perfect crystalline value. Each sample contains 15 randomly oriented grains in such a way that different types of interfaces appear, with all types of misfit from low angle to high angles. A more detailed description of this procedure can be found in Refs. 8 and 9. For the present work we consider three model Ni samples containing the same general microstructure, but scaled to three characteristic grain diameters: 5, 12, and 20 nm. The 12 nm grain size sample has been used recently to study the atomic mechanism of GB sliding.¹⁰

All MD is performed within the Parrinello-Rahman approach,²⁰ with periodic boundary conditions and fixed orthorhombic angles. The second-moment tight-binding po-

tential of Cleri and Rosato is used for describing the atomic interactions for a model fcc Ni.²¹ For studying deformation properties a uniaxial tensile stress is applied at 300 K. For the 5 nm sample a stress of 1.5 GPa was used and, for the 12 and 20 nm samples, 2.6 GPa. After an initial transient period, the strain rate can be approximated by a linear function of time, dropping to value of $4 \times 10^6/s$ after 300 ps of deformation for the 12 nm sample. To analyze the grain boundaries we calculate the local crystalline order according to the Honeycutt analysis,²² a technique based on determining the configuration of the common neighbors of a selected atom pair. For more details about this procedure applied in our simulations we refer to Ref. 9. Using this analyzing technique we defined four different classes of atoms to which different colors are attributed: gray represents fcc atoms, red represents first-nearest-neighbor hcp-coordinated atoms, green represents other 12-coordinated, and blue represents non-12 coordinated atoms. For black and white figures, light gray represents fcc atoms and black represents the other classes. This tool proved to be very helpful in the visualization of the grain boundary structures and is helpful in identifying twin planes and stacking faults.^{7,8,10}

III. EMISSION OF PARTIAL DISLOCATIONS

We will consider dislocation activity occurring in grain 13 for the three scaled samples of average grain diameters 5, 12, and 20 nm. In particular we consider the interface between grains 13 and 12. Figure 1(a) shows a section of the GB 12-13, including part of the triple junction (TJ) involving grain 1, for the loaded 12 nm grain size sample just at the onset of plastic deformation. Such a configuration will be referred to as the elastically deformed case. The view is along a $[1\bar{1}0]$ direction of grain 13, where for this grain the unit cell has been highlighted in yellow. The grain boundary plane is close to a $(1,\bar{1},13)$ plane of grain 13 and the tilt angle between the observed (111) planes in grain 13 and 12 is approximately 24° . Figure 2(a) is now a view along a (111) plane of grain 13, in which the GB plane is not so far from the plane of the page. The displayed (111) planes of both grains are highlighted in Fig. 1(a), by a single black line passing through both grains. From this viewing orientation, a twist angle of approximately 18° is found.

The GB structure has to accommodate the above mentioned misfit through a GB dislocation (GBD) network. This is evidenced in Fig. 1(a) where a clear coherence across the GB between a set of (111) planes in grain 12 and in grain 13 is seen, separated by GBD's indicated by yellow circles. For this orientation, the extra (111) plane identifying the GBD is in grain 13. Such GBD's will be referred to as GBD's of type A. Figure 3(a) now shows another view of this GB. The atoms of grain 13 contained in this view are those from the (111) planes indicated by the two black arrows in Fig. 1(b), numbered as 1. The viewing direction of Fig. 3(a) is also indicated by the black arrow numbered as 2. This viewing direction is along the $[1\bar{1}0]$ axis of grain 12, which is also not far from a similar direction in grain 13, as can be seen from the indicated unit cells. Two GBD's can be observed in

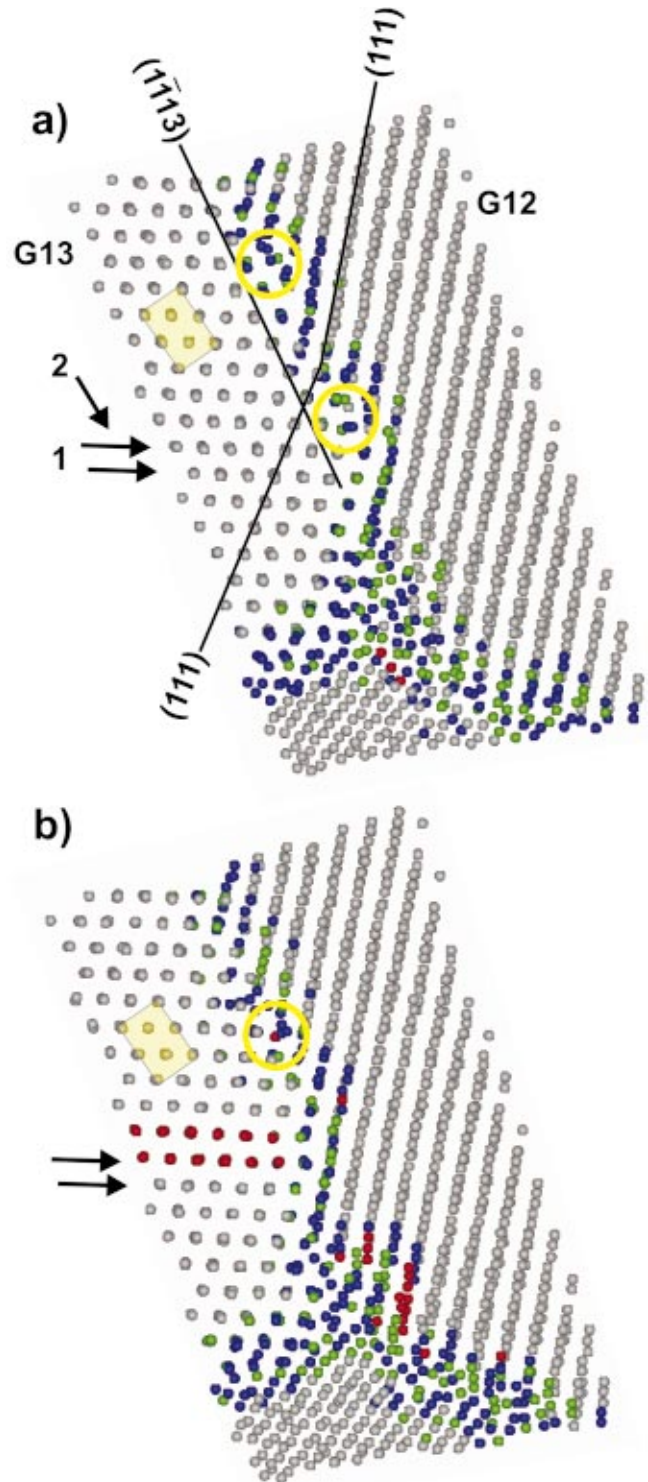


FIG. 1. (Color) View of a grain boundary in the 12 nm sample for (a) the configuration at elastic loading and (b) the configuration at a plastic strain of 2.3%. Grain boundary dislocations (of type A) that accommodate the misfit between the grains are highlighted by yellow circles.

this orientation. To guide the eye, lines that connect the (110) planes across the GB are drawn on the plots. These are referred to as GBD's of type B and, in this case, are identified by an extra $(11\bar{2})$ plane in grain 12. Thus the GBD

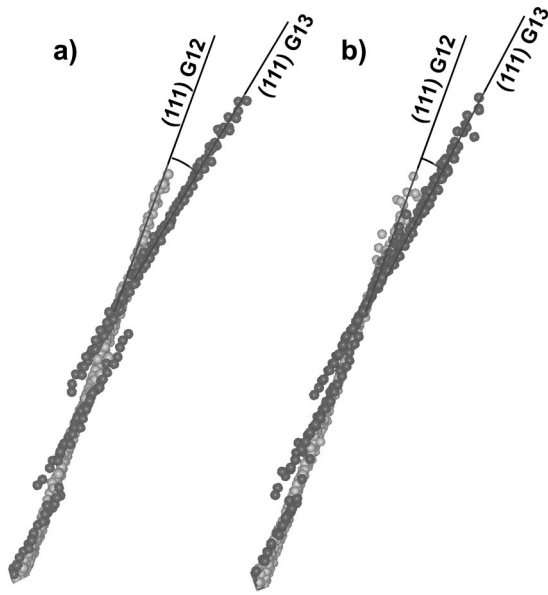


FIG. 2. A view of a few (111) planes of grain 12-13 (a) at elastic loading and (b) at 2.3% plastic strain.

network within this GB consists of at least two GBD types: A and B.

To identify a specific GB Burgers vectors for a general GB and relate it to a lattice dislocation Burgers vector remains an unclear task. For such GB's, the GBD's are expected to be less localized²³ when compared to lattice dislocations, and therefore the corresponding local Burgers vector content will be different from those of lattice Burgers vectors. Furthermore, structural disorder and the smallness of the nanoscale GB planes make it difficult for an accurate Burgers vector content analysis using, for example, the Frank-Bilby equation.²⁴

During deformation of this sample, the GBD of type A (in Fig. 1), which is closest to the TJ, dissociates into a Shockley partial, traveling through grain 13. This can be seen in Fig. 1(b), showing the same GB after 2.3% plastic strain, in which this GBD has annihilated. The two (111) planes, of red hcp atoms indicate the intrinsic stacking fault left behind when the partial is traveling through grain 13. Since the Burgers vector of the lattice dislocation is not the same as the Burgers vector of the GBD, other types of local changes are to be expected in the GB. We will now show that the emission of the partial occurs along with local changes in GB orientation, GB structure, and GBD distribution.

The atomic mechanism behind this dislocation emission is the following: during deformation sliding is observed in all GB's, including GB 12-13. In previous work¹⁰ we have identified the atomic-scale activity associated with GBS's as consisting of atomic shuffling and stress assisted free volume migration. In the case of GB 12-13 the free volume migrates from the nearby triple junction and diffuses under the applied stress towards the GBD of type A nearest to the TJ [Fig. 1(a)]. Or, equivalently, two atoms from the core region of the GBD migrate to nearby positions within the GB. The stress-assisted diffusion of free volume originating from a TJ line is shown in Fig. 4. Here, a view perpendicular to GB 12-13 is

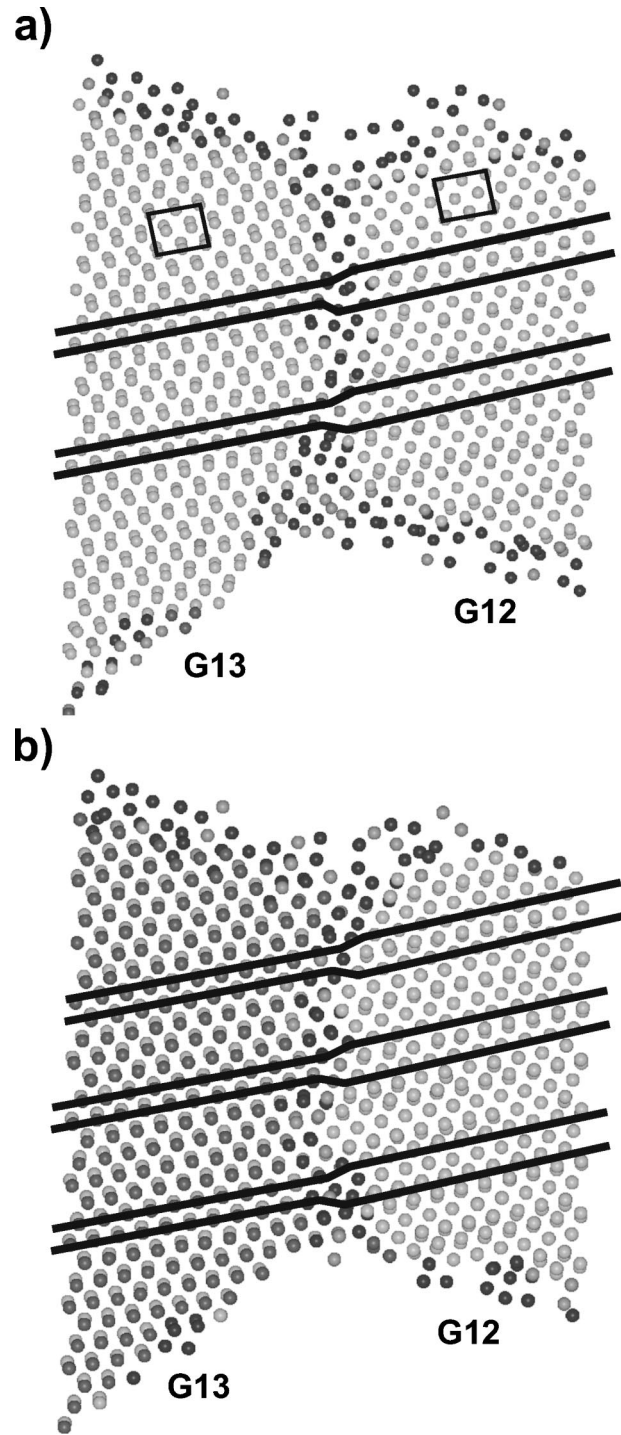


FIG. 3. Section of grain boundary 12-13 indicated in Fig. 1 with arrows numbered 1 and in a viewing direction given by the arrow numbered 2. The [110] unit cells are shown for both grains.

given. For clarity, the fcc atoms are not shown and thus only the GB atoms can be seen. The blue dashed line represents the surrounding TJ region. The atomic positions are those after the emission of the partial and thus the double hcp planes of the stacking fault can be seen. Additionally, the figure shows the regular pattern of the GB structure which, although not a special coincidence site lattice (CSL) structure, still shows significant order. Atomic displacements big-

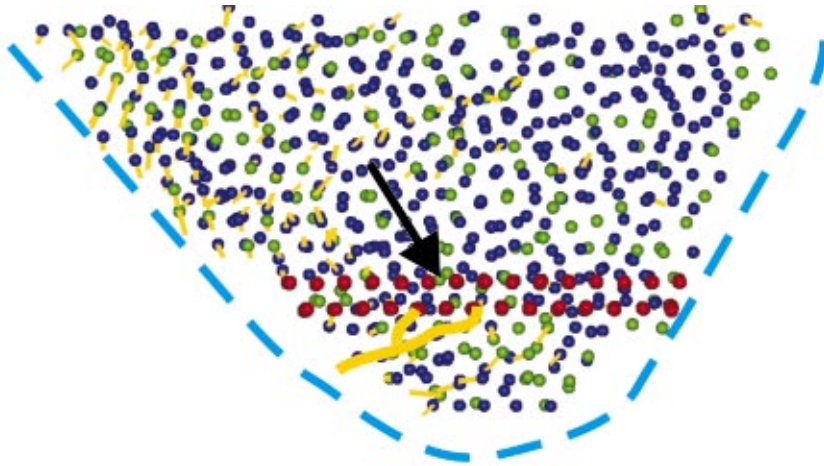


FIG. 4. (Color) Grain boundary 12-13 from which the partial dislocation nucleates. Only non-fcc atoms are shown for the configuration at 2.3% plastic strain. The dark yellow vectors ($>1.2 \text{ \AA}$) represent the atomic displacement after elastic deformation. The dashed blue line indicates the surrounding triple-junction regions. The black arrow indicates the region in which the dislocation nucleates. Stress-assisted free volume migration is observed (the thicker dark yellow lines) from a nearby triple-junction region.

ger than 1.2 \AA between the elastically and plastically deformed (after dislocation emission) configurations are displayed in dark yellow. The black arrow indicates where the partial has nucleated, and the thicker dark yellow lines indicate the path where the free volume migrates from the TJ to the corresponding GBD region. Figures 5(a) and 5(b) show a closeup of the GB for the same two configurations with the viewing direction the same as that in Fig. 1. Only

the atomic positions of the (111) planes that become the stacking fault are shown together with some GB atoms. In Fig. 5(a) the positions are those of the elastically deformed sample, and in Fig. 5(b), those of the plastically deformed sample. The displacement vectors of all the surrounding atoms are also shown. The free volume migration can be identified by the larger displacement vectors in the GB beginning at a nearby TJ (not shown) and ending at the lattice dislocation nucleation/GBD region. Or alternatively, at the end of this replacement sequence where the dislocation nucleates, two atoms move in a direction towards grain 12, demonstrating that a local shuffling of atoms around the GBD allows the creation of the necessary Burgers vector for the Shockley partial. It is interesting to note that the partial does not propa-

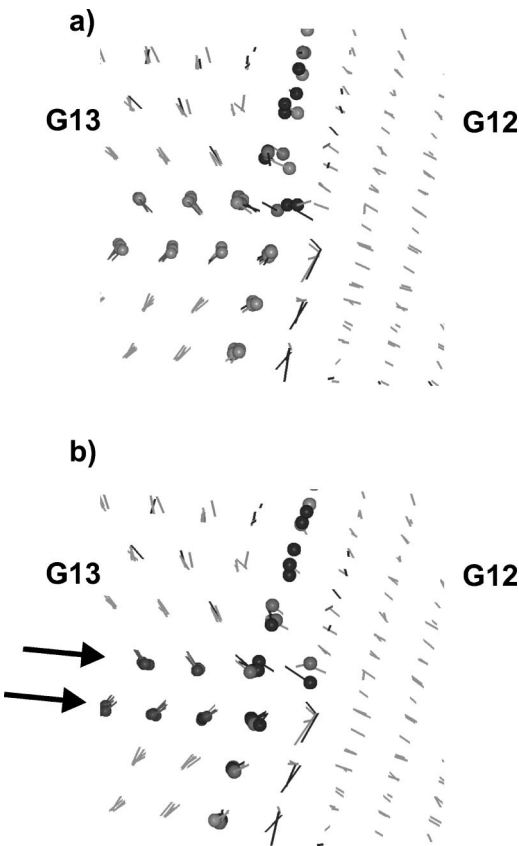


FIG. 5. Close up of Fig. 1 showing only the grain boundary atoms and the partial lattice dislocation (a) after elastic deformation and (b) after 2.3% plastic strain. The displacement vectors of all the surrounding atoms are also shown. Two atoms from the grain boundary/dislocation nucleation region move into grain 12.

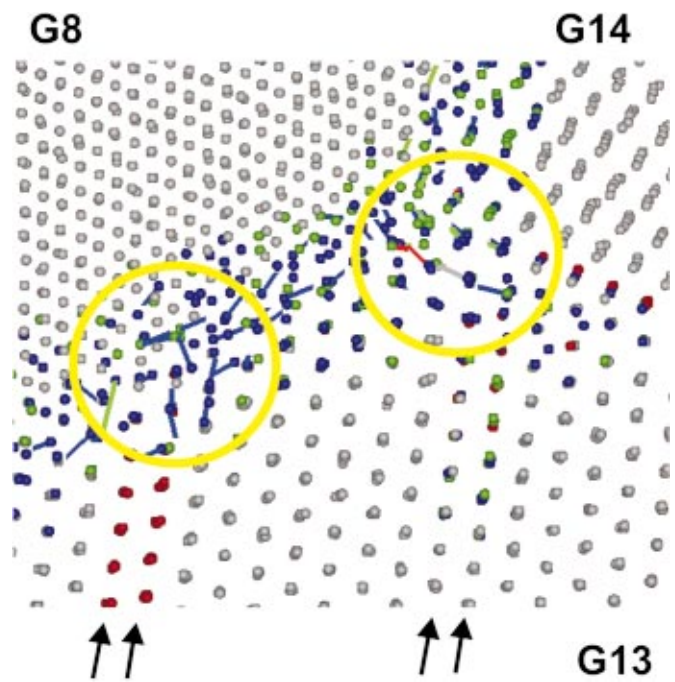


FIG. 6. (Color) Triple junction 8-13-14 for the 20 nm sample at 2.7% plastic deformation. The atomic displacements corresponding to the plastic deformation are also shown. Atomic activity can be seen between the nearby triple junction and the two nucleation regions which occur slightly below the displayed plane of atoms.

gate immediately; nucleation and propagation are separated in time by about 10 ps during which a small amount of structural relaxation occurs around the nucleation point.

Upon dislocation emission, the resulting slip induces a reorientation of the grain and thus also the misorientation of GB 12-13. In part this is reflected by the removal of a dislocation of type A. Also, when looking along the (111) plane in Figs. 2(a) and 2(b) [where Fig. 2(b) shows the same atoms at 2.3% strain] it can be seen that after the emission of the partial a local reorientation of the (111) planes of grain 13 allows the reduction of the twist angle. Inspection of Figs. 3(a) and 3(b) shows that there is also a redistribution of GBD's of type B. Before deformation, two type-B GBD's are seen, and after partial dislocation emission and the removal of a GBD of type A, there is also the creation of an additional GBD of type B, rearranging in the same time the other type-B dislocations already present in that GB.

The emittance of the partial and the incorporation of the GBD type B induces local reorientation generating a new intrinsic interface structure which differs from the initial structure because of a change in total Burgers vector content. Close examination of the GB structure shown in Figs. 1 and 3 shows that the GB structure tends to be more faceted after the emission of the partial, which indicates that this mechanism lowers the total energy of the GB. The tendency of GB ordering during grain boundary sliding triggered by atomic shuffling and stress-assisted diffusion has also been discussed recently in Ref. 25. These results suggest the beneficial effect of GB disorder in the mechanism of plastic deformation of nanosized GB's, but they also suggest the presence of a hardening mechanism during plastic deformation. In Ref. 25 we further showed that the cohesive energy distribution of the GB atoms shifts to more negative values as a result of the tensile loading and unloading cycle.

As mentioned, an increased dislocation activity is observed when the grain size increases from 12 to 20 nm. For the 20 nm sample a similar mechanism for the emission of the partials is observed. Figure 6 shows the triple-junction region between grains 8, 13, and 14. Roughly perpendicular to the viewing direction and below the displayed atoms is GB 12-13. Figure 6 shows the displacements of the atoms between the elastically deformed configuration and that at 2.7% of plastic strain. Between these configurations two partials (indicated by the red stacking fault) have been emitted. The first dislocation is emitted from GB 12-13 very close to the triple junction with grain 8. This process of emittance is very similar to the one described in the former paragraph in the 12 nm sample. The second partial is emitted at the triple junction between grains 12, 13, and 14. Both nucleation regions are indicated by open yellow circles. Here, free volume is "squeezed" out of the nearby quadrupole between grains 8, 12, 13, and 14, which then migrates to the misfit region between grains 13 and 14. Figures 7(a) and 7(b) show GB 12-13 in the same viewing direction as the one in Fig. 1. The elastically deformed configuration is given in (a) and shows the presence of five GBD's, highlighted by the black circles. The configuration after the emission of the partials is given in (b) and it shows that there are only three GBD's left. It is clearly shown that both nucleations of partial lattice disloca-

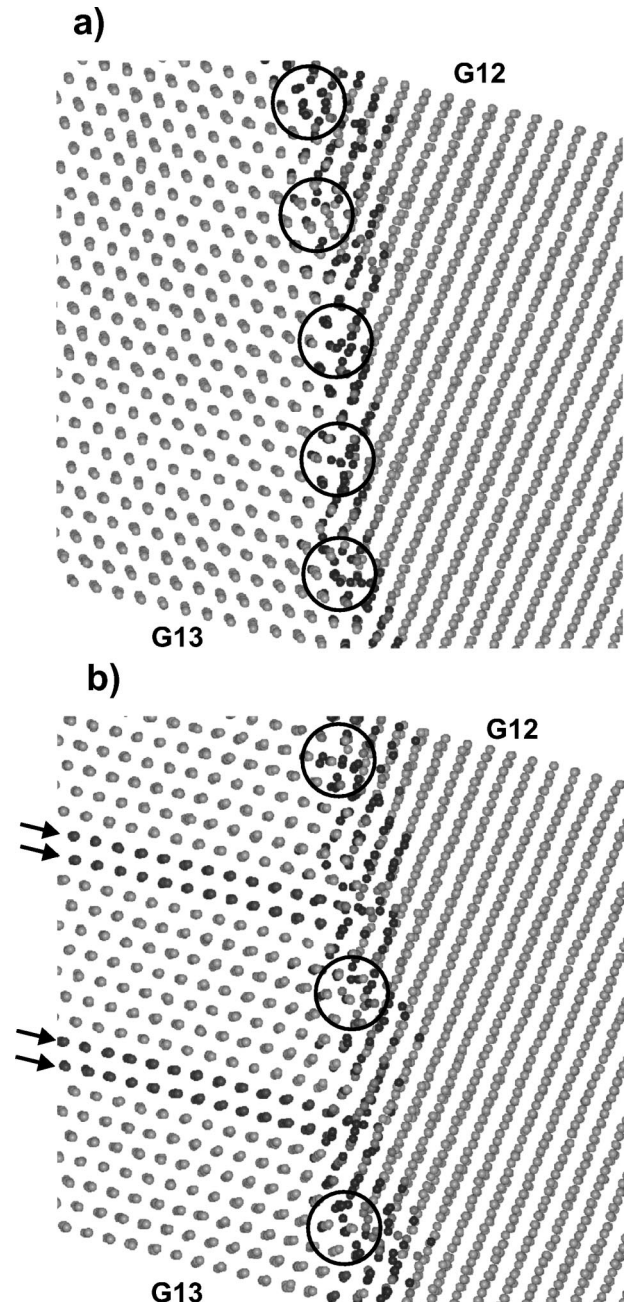


FIG. 7. (a) The elastically deformed configuration and (b) the 2.7% strain configuration for the GB 12-13 in the 20 nm sample is shown. The viewing direction is the same as in Fig. 1. For the elastically deformed configuration, five grain boundary dislocations are identified, which, upon the nucleation of two partial lattice dislocations, reduce to three.

tions involve dissociation of GBD and modification of the remaining GBD distribution. The emittance of the partials also induces structural relaxation and changes in the GBD's in GB 13-14. This is shown in Figs. 8(a) and 8(b). GB 13-14 has an orientation not far from a perfect twin, and therefore the GB relaxed to the twin plane-stair structure as is described in Refs. 8,10 and 25. The plot views the GB slightly off along the twin planes which are indicated by the right horizontal arrow in Fig. 8(b) and visualized by a (111) plane

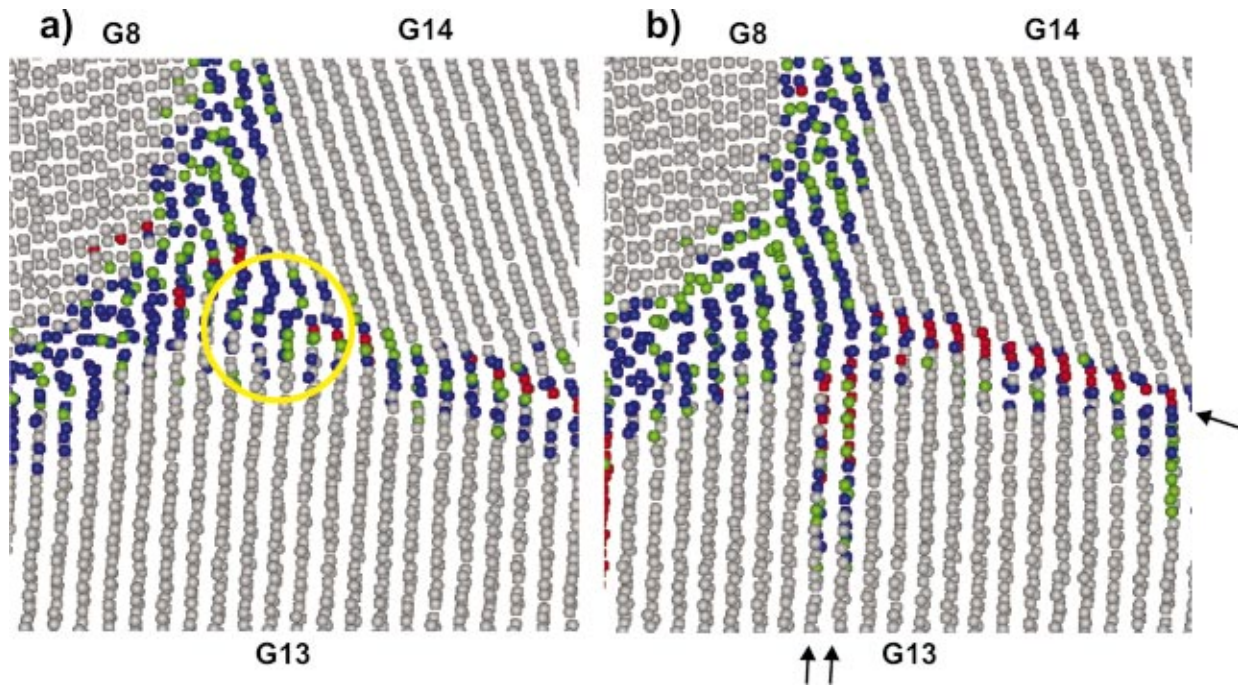


FIG. 8. (Color) (a) Same section as that in Fig. 6 with a slightly different viewing orientation. A grain boundary dislocation is highlighted with a yellow circle.

of red atoms. Before the partial is emitted, the GB contains a GBD close to the triple junction, where the associated (111) plane in grain 13 have been indicated by the open yellow circle in Fig. 8. After emission, this GBD disappears and the twin plane relaxes to a more ordered configuration. The latter is demonstrated by the presence of a larger single red plane after dislocation emission.

We now view the same GB 12-13 but in the scaled sample with a mean grain size of 5 nm, in which no dislocation activity is observed. The plastic deformation is fully accommodated in the GB: only GBS is observed, which is facilitated by atomic shuffling and stress-assisted free volume migration. Figures 9(a) and 9(b) show the GB between grains 12 and 13 prior to deformation and at 2.8% total strain in the same orientation as Fig. 1 for the 12 nm sample. Similar GB dislocations of type A can be observed that are necessary for accommodating the misfit between the (111) planes. Upon deformation, however, the GBD can move upwards by a shuffling of atoms without the emission of a partial dislocation. In order to make this more clear, we have numbered the (111) planes in Fig. 9 for both grains 12 and 13. Before deformation, the GBD is situated between row 8-10 of grain 13 and row 2-3 of grain 12. During deformation the GBD climbs to 6-8 of grain 13 and 1-2 of grain 12. Careful examination of the atomic displacement demonstrates a lot of shuffling and in one case a free volume migration under the applied stress. Moreover, the sliding induces GB migration: comparing Fig. 9(b) with 9(a), it can be seen that before deformation plane 4 in grain 12 had the orientation of the (111) planes of grain 12, whereas at 2.8% load, this plane has taken partly the orientation of the (111) planes in grain 13.

IV. DISCUSSION

That GB's act as sinks for lattice dislocations under the action of applied stress is a well established property, but it is also known that the opposite mechanism, i.e., emission of lattice dislocations from GB's is also possible.^{23,26} A few possible dislocation reactions that lead to the emission of partials from a GBD are discussed in Ref. 27. There is, however, no detailed understanding of the emission process and of the local changes in GB structure accompanying the emission. This is mainly due to the fact that these kinds of observations can only be done in a high-resolution electron microscope, a method that needs a thin-film or wedge-like geometry, making it very difficult to distinguish among intrinsic properties and sample geometry artifacts.^{6,28}

Valiev *et al.*²³ suggested that the Burgers vector of the lattice dislocation may be obtained in the GB by the summation of small Burgers vectors of GBD's; i.e., a lattice dislocation may be formed by association of GBD's. As a matter of fact, this is the opposite process of what was suggested by Gleiter²⁶ for core spreading when a lattice dislocation is absorbed in a GB.

In previous work⁸ we have shown that GB's in nanocrystalline samples show ordered structures that are not different from what is known in coarse-grained materials, including features such as GBD and GB steps. We have also shown that localized activated atomic processes, identified as atomic shuffling and stress-assisted free volume migration, are the stress relaxation mechanisms that facilitate the GBS. An important observation in this paper is that the precursor to the nucleation of lattice dislocations in the regions of misfit is a similar atomic activity. Indeed, our results show that

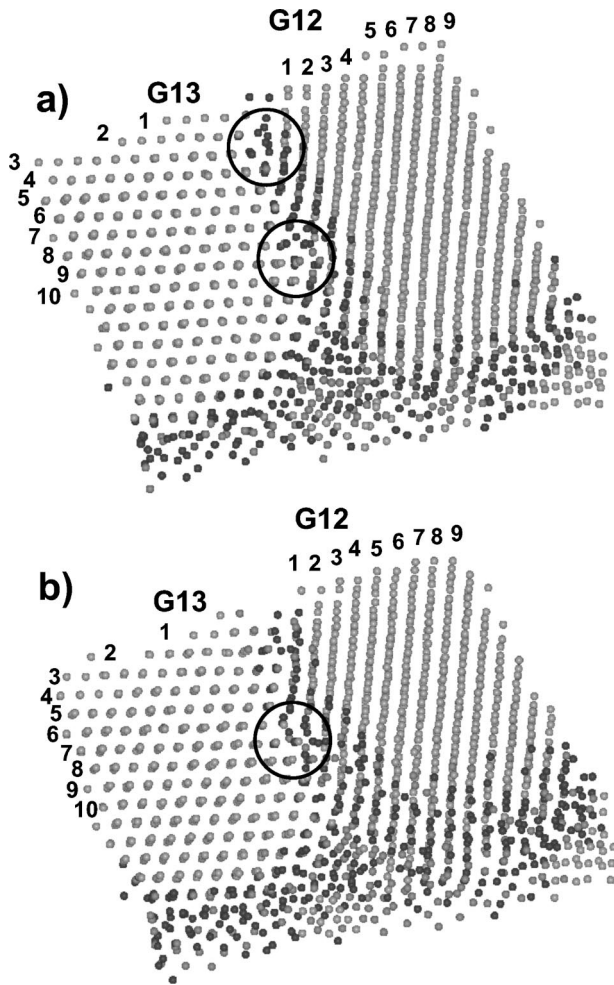


FIG. 9. The grain boundary between grains 12 and 13 of the 5 nm grain size sample prior to loading (a) and at 2.8% total strain (b) in the same orientation as Fig. 1 for the 12 nm sample.

local atomic shuffling often involving stress-assisted diffusion of free volume from a nearby TJ to the region of misfit surrounding a GBD allows the “formation” of the Burgers vector of a partial lattice dislocation (PLD), resulting in a dissociation of the GBD. This is the first time a direct link between the GBS process, its associated atomic scale activity, and the nucleation of an initial PLD from the GBD has been observed.

We further demonstrated that the generation of the PLD, in which the Burgers vector is different to the observed GBD. In other words, a GB of a certain GBD content transforms to a lattice partial dislocation and a GB of another GBD content. It is worth to note that in the 12 nm sample, a short elapsed time is observed between the generation of the partial and the propagation of the partial, suggesting that the stresses necessary for the two processes are different and/or the importance of the local relaxation of the GB by generation of the PLD. Upon subsequent propagation of the PLD further structural relaxation within the GB region takes place, especially at these regions where the partial dislocation impinges on the GB’s. The resulting slip across the grain

can be accommodated in the GB’s leading to changes in the misorientation of neighboring grains and thus further structural changes at atomic level.

These observations address the questions of (1) why no partials are observed in samples with grain sizes of 5 nm and (2) why only partial dislocations are seen and not full dislocations in 3D samples with grain sizes up to 20 nm. We suggest that the answer to both questions lies in the atomic activity that is observed in the GB’s during deformation and that accompanies the creation and the propagation of the PLD. In the present work, many of the regions of misfit seen in the 12 and 20 nm sample also exist in the scaled 5 nm grain size sample, however, as expected, no dislocation activity is observed. What is seen is significantly more atomic-scale activity for a given plastic strain within the GB and TJ regions. We propose that the regions of misfit, the GBD’s, are less localized in the 5 nm sample compared to the 12 and 20 nm sample due to spatial restrictions. We emphasize that, by this, we do not suggest that a fundamental change in GB structure occurs with a reduction in grain size, but rather the level and density of connectivity in terms of misfit regions leads to more delocalized GBD’s. Delocalization hinders dislocation nucleation by association of GBD’s but favors a climb of the GBD by local shuffling and stress-assisted free volume migration and, thus, the GBS mechanism for plastic deformation. Moreover, the extensive atomic activity can lead to a reduction of shear across grains and thus further reduce the likelihood of dislocation activity.

On the other hand, with increasing grain size, an increase in partial dislocation nucleation is seen, with several partials nucleating in different regions of misfit in a GB, rather than the emission of any trailing partial constituting a full dislocation. Important to note is that even at 20 nm grain sizes, the contribution of the partials to the observed plasticity is minor, compared to the contribution from the GB sliding triggered by the atomic activity. With subsequent GB relaxation and changes in GBD array distributions during the generation of the partial, especially in the vicinity of the GBD from which a dislocation has nucleated, it becomes increasingly clear that from a structural and energetical perspective, there is no *a priori* reason for the emission of the second trailing partial. This in turn opens the question of whether or not partial dislocations at these grain sizes need to be seen as precursors to a full dislocation. In the 2D columnar work of Yamakov *et al.*,¹⁶ full dislocations are seen. However, we caution in generalizing these observations to the more realistic case of a fully 3D GB network, where many more slip planes are active and the accommodation mechanism may be quite different. In any event, the energetics of a full dislocation — or rather the leading and trailing partial, and the corresponding stacking fault defect — is expected to be quite different in a three-dimensional grain where the dislocation core line is pinned at both ends to a general GB, compared to an essentially 2D infinitely extended dislocation structure.

V. CONCLUSION

In conclusion, we have provided a number of examples, in which we have identified the nucleation of a partial lattice

dislocation from a GBD. The nucleation process is facilitated by atomic shuffling and often by the emission of free volume from a nearby TJ—in other words, the same atomic activity which has also been identified as constituting the GB sliding process. The nucleation and propagation induce changes in the resultant GBD distribution and additional structural relaxation is observed in the GB and nearby TJ. From a temporal analysis there is an indication that nucleation and propagation are separated in time. For increased grain diam-

eters, an increase in partial dislocation activity is seen, but no full dislocations are observed probably due to subsequent structural relaxation after the emission of the partial. At smaller grain sizes, the same GBD's are observed. They undergo significantly more atomic-scale activity resulting in a climb of the GBD without the generation of partials, suggesting that GBD's are more delocalized and therefore GBD motion by atomic shuffling is facilitated and the association of GBD's into a partial dislocation is hindered.

-
- ¹E. O. Hall, Phys. Soc. London, Sect. B **64**, 747 (1951).
²N. J. Petch, J. Iron Steel Inst., London **174**, 25 (1953).
³J. R. Weertman, in *Nanostructured Materials: Processing, Properties, and Potential Applications* (William Andrew, Norwich, NY, 2002).
⁴C. J. Youngdahl, R. X. Hugo, H. Kung, and J. R. Weertman, in *Structure and Mechanical Properties of Nanophase Materials—Theory and Computer Simulation vs. Experiment*, edited by D. Farkas, H. Kung, M. Mayo, H. Van Swygenhoven, and J. Weertman, MRS Symposia Proceedings No. 634 (Materials Research Society, Pittsburgh, 2000).
⁵S. X. McFadden, A. V. Sergueeva, T. Kruml, J.-L. Martin, and A. K. Mukherjee, in *Structure and Mechanical Properties of Nanophase Materials—Theory and Computer Simulation vs. Experiment* (Ref. 4).
⁶P. M. Derlet and H. Van Swygenhoven, Philos. Mag. A **82**, 1 (2001).
⁷H. Van Swygenhoven, M. Spacer, and A. Caro, Acta Mater. **47**, 3117 (1999).
⁸H. Van Swygenhoven, D. Farkas, and A. Caro, Phys. Rev. B **62**, 831 (2000).
⁹H. Van Swygenhoven and A. Caro, Phys. Rev. B **58**, 11 246 (1998).
¹⁰H. Van Swygenhoven and P. M. Derlet, Phys. Rev. B **64**, 224105 (2001).
¹¹H. Van Swygenhoven, P. M. Derlet, A. Caro, D. Farkas, M. J. Caturla, and T. Diaz de la Rubia, in *Structure and Mechanical Properties of Nanophase Materials—Theory and Computer Simulation vs. Experiment* (Ref. 4).
¹²J. Schiøtz, F. D. Di Tolla, and K. W. Jacobsen, Nature (London) **391**, 561 (1998).
¹³J. Schiøtz, T. Vegge, F. D. Di Tolla, and K. W. Jacobsen, Phys. Rev. B **60**, 11 971 (1999).
¹⁴V. Yamakov, S. R. Phillpot, D. Wolf, and H. Gleiter, in *Computer Simulations in Condensed Matter Physics*, edited by D. P. Landau, S. P. Lewis, and H.-B. Schtler (Springer, New York, 2000), Vol. XIII, p. 195.
¹⁵V. Yamakov, D. Wolf, S. R. Phillpot, and H. Gleiter, Acta Mater. **50**, 61 (2002).
¹⁶V. Yamakov, D. Wolf, M. Salazar, S. R. Phillpot, and H. Gleiter, Acta Mater. **49**, 2713 (2001).
¹⁷P. Keblinski, D. Wolf, S. R. Phillpot, and H. Gleiter, Scr. Mater. **41**, 631 (1999).
¹⁸A. P. Sutton and R. W. Balluffi, *Interfaces in Crystalline Materials* (Clarendon, Oxford, 1995), Chap. 9.
¹⁹G. Z. Voronoi, J. Reine Angew. Math. **134**, 199 (1908).
²⁰M. Parrinello and A. Rahman, J. Appl. Phys. **52**, 7182 (1981).
²¹F. Cleri and V. Rosato, Phys. Rev. B **48**, 22 (1993).
²²D. J. Honeycutt and H. C. Andersen, J. Phys. Chem. **91**, 4950 (1987).
²³R. Z. Valiev, V. Yu. Gertsman, and O. A. Kaibyshev, Phys. Status Solidi A **97**, 11 (1986).
²⁴See, for example, Secs. 2.3 and 2.4 of Ref. 18.
²⁵A. Hasnaoui, H. Van Swygenhoven, and P. M. Derlet, Acta Mater. (to be published).
²⁶H. Gleiter, Prog. Mater. Sci. **25**, 125 (1981).
²⁷J. P. Hirth, Metall. Trans. A **3**, 3047 (1972).
²⁸L. E. Murr, Mater. Sci. Eng. **51**, 71 (1981).